 doi:10.20944/preprints202203.0090.v1

Type of the Paper (Article)

Strong Coupling between A Single Quantum Emitter and A Plasmonic Nanoantenna on A Metallic Film

Shun Cao [1], Yuwei Sun [1], Zhenchao Liu [1] and Sailing He [1,2,3*]

[1] Centre for Optical and Electromagnetic Research, National Engineering Research Center for Optical Instruments, Zhejiang University, Hangzhou 310058, China; caoshun@zju.edu.cn(S.C.); sunyuwei@zju.edu.cn(Y.S.); lzc_archer@zju.edu.cn(Z.L)
[2] Ningbo Research Institute, Zhejiang University, Ningbo 315100, China
[3] Department of Electromagnetic Engineering, School of Electrical Engineering, KTH Royal Institute of Technology, S-100 44 Stockholm, Sweden
* Correspondence: sailing@kth.se

Abstract: The strong coupling between individual quantum emitters and resonant optical micro/nanocavities is beneficial to understand light and matter interactions. Here we propose a plasmonic nanoantenna placed on a metal film to achieve an ultra-high electric field enhancement in the nanogap and ultra-small optical mode volume. The strong coupling between a single quantum dot and the designed structure is investigated in detail by both numerical simulations and theoretical calculations. When a single QD is inserted into the nanogap of the silver nanoantenna, scattering spectra show remarkably large spectral splitting and typical anti-crossing behavior of the vacuum Rabi splitting, which can be realized in the scattering spectra by varying the nanoantenna thickness. Our work shows a possible way to enhance light-matter interaction at a single quantum emitter limit, which can be useful for future quantum and nanophotonic applications.

Keywords: strong coupling; nanoantenna; single quantum dot

1. Introduction

Recently, the interactions between the emitters and an optical micro/nano cavity have attracted huge interest[1-4]. The strong coupling to approach the single-photon limit between individual quantum emitter and optical cavity, which can be described by cavity quantum electrodynamics (QED), is of particular interest and enabling multiple optical applications in efficient single-photon sources, quantum information processing[5, 6], quantum communication[7, 8], low threshold lasers[9] and ultrafast optical switch[10]. Strong coupling can be manifested in the optical spectrum of the hybrid structure as vacuum Rabi splitting. The coupling strength, g, of the interaction is proportional to the ratio of the quality factor, Q, of the optical cavity to the mode volume, V. Therefore, one method to achieve strong coupling is by using dielectric optical cavities with high Q modes, for example, micropillars[11], photonic crystals[12, 13], metasurfaces[14-16]. Obtaining such a high-quality factor requires complex experimental fabrication techniques or demanding experimental conditions such as cryogenic temperatures. Also, the coupling strength g depends on the local electric field. The higher the local electric field leads to the greater the coupling strength[14]. Cavities made of metal materials that can support surface plasmons (SPs) can focus electromagnetic fields into deep sub-wavelength mode volumes[17, 18]. Therefore, utilizing such cavities can simplify the experimental conditions for strong interactions between light and matter and may allow quantum optical experiments to be carried out under ambient conditions.

At visible wavelengths, noble metals, such as gold and silver, are used to construct micro/nano structures supporting SPs in many applications [19-21]. Although the Q factor

Preprints (www.preprints.org) | NOT PEER-REVIEWED | Posted: 7 March 2022 doi:10.20944/preprints202203.0090.v1

of the SP mode is relatively low compared with photonic cavities, their optical volume can be drastically reduced. Many research have been conducted to study the interactions between SPs modes and quantum emitters. In recent years, strong coupling have also been observed by using plasmonic gold dimers[22][22], silver nanorod[23], silver nanoprism[24], etc. Hundreds of quantum emitters or more were involved in these experiments. However, for quantum information processing, one needs to reach the limit of a single emitter coupled to the cavity. H. Groß *et al* realized strong coupling between a scanning plasmonic nanoresonator probe and a single semiconductor QD under ambient conditions[25]. K. Santhosh *et al* demonstrated that the coupling rate can be close to the strong coupling regime when placing a single QD in the nanogap of a silver bowtie[26]. By further increasing the local electric field enhancement and reducing the optical mode volumes, one can indeed achieved strong coupling between individual quantum emitter and micro/nanocavities.

In this work, a plasmonic nanoantenna placed on a metal film is proposed, which exhibits ultra-high electric field enhancements in the nanogap and ultra-small optical volume. Strong coupling between a single quantum dot and the designed structure can be achieved. When single QD is inserted into the nanogap of the silver nanoantenna, scattering spectra show distinct spectral splitting and the vacuum Rabi splitting can be upto 188 meV. Both the FDTD simulations and coupled-mode theory (CMT) analysis confirm the strong coupling regime is approached in the hybrid system. Our work offers a new way to realize strong light-matter interactions at single quantum emitter limit, which can be useful for quantum and nanophotonic applications.

2. Materials and Methods

The scattering spectra of the silver nanoantenna placed on the silver film and the substrate and the hybrid structures were numerically simulated by using three-dimensional (3D) FDTD (Lumerical FDTD Solutions).

The refractive index of silver was obtained from data by Johnson and Christy[27]. The permittivity of the QDs was approximately given by a Lorentz oscillator model:

$$\varepsilon(\omega) = \varepsilon_{\infty} + \frac{f\omega_0^2}{\omega_0^2 - \omega^2 - i\Gamma_0\omega} \quad (1)$$

where ε_∞, f, ω_0 and Γ_0 are the high-frequency dielectric constant, the oscillator strength, the exciton transition frequency and the exciton linewidth, respectively. In this work, these parameters were chosen as $\varepsilon_\infty = 6.1$, $f = 0.6$, $\omega_0 = 1.879$ eV, and $\Gamma_0 = 80$ meV[26].

A Total Field Scattered Filed (TFSF) source with TE-polarized (polarization along the y-axis) is used to calculate the scattering spectra of the designed structures. Perfectly matched layer (PML) boundary conditions are employed surrounding the whole structures. A finer mesh region with size of 0.5 × 0.5 × 0.5 nm3 was applied in the nanogap while a coarser meshing with size of 1 × 1 × 1 nm3 was applied elsewhere.

3. Results and Discussion

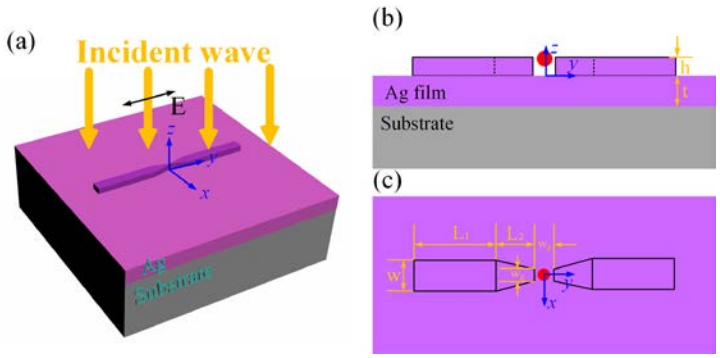

Figure 1. (a) Schematic diagram of the proposed silver nanoantenna on a silver film. (b) Side view of the structure in the y-z plane. (c) Top view of the structure in the x-y plane.

Preprints (www.preprints.org) | NOT PEER-REVIEWED | Posted: 7 March 2022 doi:10.20944/preprints202203.0090.v1

3.1. The proposed plasmonic nanoantenna on a metal film

Figure 1 schematically shows the designed structure, which comprises plasmonic nanoantenna, a metal (silver) film and a substrate. The perspective, side and top view of the structure are depicted in Fig. 1(a), 1(b) and 1(c), respectively. The coordinate system and parameters of the structure were also given in these figures. As shown in Fig. 1(a), the plasmonic nanoantenna is made up of two identical parts, which both have a cuboid and four trustum of pyramid. The parameters denotations are shown in Fig. 1(b) and 1(c). The thickness of this nanoantenna is h. A nanogap is formed between two parts of the nanoantenna with length g and width w_g. These two parameters have same values. The length and width of the rectangle is L_1 and w, and the height of trapezoid is L_2. In this work, the material of the plasmonic nanoantenna is chosen as silver due to its relatively low losses and hence higher quality factor Q when compared with other metal materials. The thickness of silver film is t = 200 nm, which is thick enough to block the incident wave to transmit the structure. The above structures are placed on the silica (n = 1.47) substrate. By varying the structural parameters of the nanoantenna, the resonance of the localized SP can be tuned. In order to support resonant mode with ultra-large electric field enhancements and ultra-small optical volumes in the nanogap, the parameters of the silver nanoantenna are chosen as follows: L_1 = 370 nm, L_2 = 126 nm, w = 70 nm, and w_g = 7 nm. Consequently, when a single quantum emitter was inserted into the nanogap, strong coupling between the plasmonic nanoantenna and the quantum emitter can be achieved.

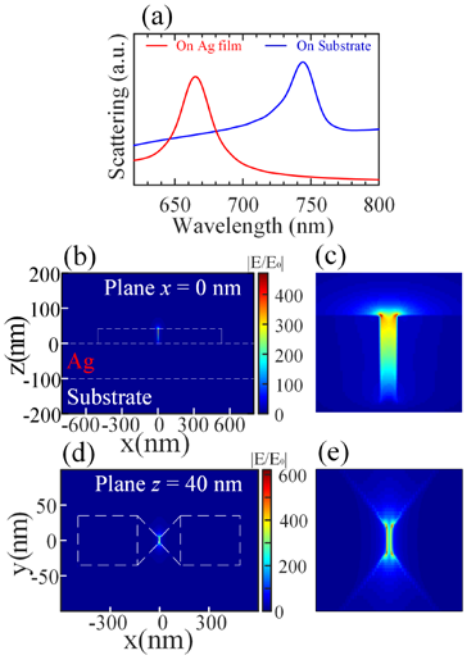

Figure 2. (a) Simulated scattering spectra of the silver nanoantenna placed on a silver film (red line) and directly on a silica substrate (blue line). (b) The electric field distribution of the longitudinal mode on plane x = 0 for the silver nanoantenna placed on the silver film. (c) The magnified electric field distribution in the nanogap in (b). (d) The electric field distribution of the longitudinal mode on plane z = 40 nm for the silver nanoantenna placed on the silver film. (e) The magnified electric field distribution in the nanogap in (d). The color bars indicate the electric field enhancement.

Preprints (www.preprints.org) | NOT PEER-REVIEWED | Posted: 7 March 2022 doi:10.20944/preprints202203.0090.v1

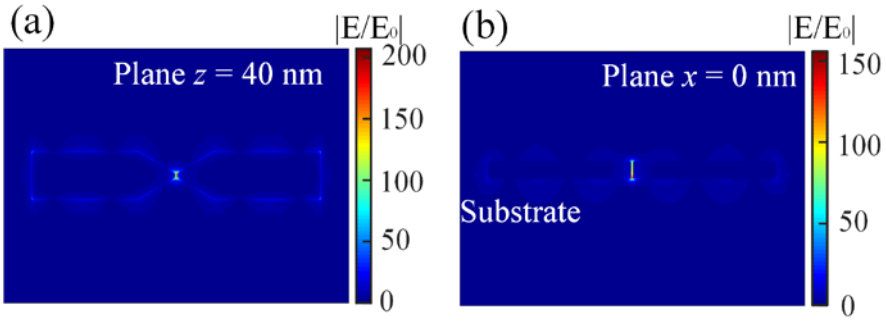

Figure 3. (a) The electric field distribution of the longitudinal mode on plane z = 0 for the silver nanoantenna directly placed on the silica substrate. (b) The electric field distribution of the longitudinal mode on plane x = 0 for the silver nanoantenna directly placed on the silica substrate. The color bars indicate the electric field enhancement.

The plasmonic behavior of the single silver nanoantenna placed on silver film and substrate directly are investigated by using finite-difference time-domain (FDTD) method (Lumerical FDTD Solutions), respectively. The detailed simulations can be found in Materials and Methods. The calculated scattering spectra are depicted in Fig. 2(a). From this figure, both under these two conditions, the structure possess longitudinal mode due to dipolar coupling between the two parts of the silver nanoantenna. When placed on the silica substrate, the blue line in Fig. 2(a) shows that the plasmonic nanoantenna supports localized SP mode at 744 nm and the Q factor is 12.6. However, for nanoantenna on silver film, the resonant frequency of the mode has a blue shift and exhibits a higher Q factor, i.e., 22.2. The electric field distributions at plane x = 0 for nanoantenna placed on silver film is shown in Fig. 2(b). It can be seen clear that the electric field is highly confined in the nanogap of the nanoantenna. Figure 2(c) shows the enlarged electric field distributions in the nanogap. Furthermore, the electric hot spot is concentrated at top of the nanogap. The electric field at vicinity of the nanoantenna has maximum value, which is enhanced ($|E/E_0|$, where E_0 is the electric field of the incident wave) as high as 470 folds. There is no remarkably electric field enhancement in the else parts of the structure. Then the electric field distributions at top plane (z = 40 nm) of the nanoantenna is drawn in Fig. 2(d). Similarly, the enlarged electric field distributions in the nanogap at this plane is shown in Fig. 2(e). When close to the four vertexes of the nanogap, the electric field is greatly enhanced and can be more than 600 times to incident wave. As depicted in Fig. 2(e), the electric field will be enhanced more than 200 times in the center of the nanogap. The calculated optical volume of the resonant longitudinal mode is ultra-small, only $1.61\times10^{-6}\ \lambda^3$ (due to the highly confined electric field in the nanogap), which is one order lower than that of a plasmonic waveguide–slit structure on a metallic substrate reported by G. Zhang *et al*[28].

In addition, the electric field distributions at plane x = 0 of the nanoantenna placed on silica substrate are shown in Fig. 3(a). It can be seen that the electric field is highly focus in the nanogap as well. However, when compared with Fig. 2(b), the electric hot spot is concentrated at bottom of the nanogap, which is different with the nanoantenna placed on the silver film. Then the electric field distributions at bottom plane (z = 0 nm) of the nanoantenna is depicted in Fig. 3(b). The electric field in the nanogap is also strongest and there are certain electric field enhancements surrounding the nanoantenna and the silica substrate. In the plane x = 0 nm, the electric field is enhanced maximum more than 150 times and this is much lower than that of the silver nanoantenna placed on the silver film. It can be found that the silver film can help more electric fields to concentrate in the nanogap of the nanoantenna.

Preprints (www.preprints.org) | NOT PEER-REVIEWED | Posted: 7 March 2022 doi:10.20944/preprints202203.0090.v1

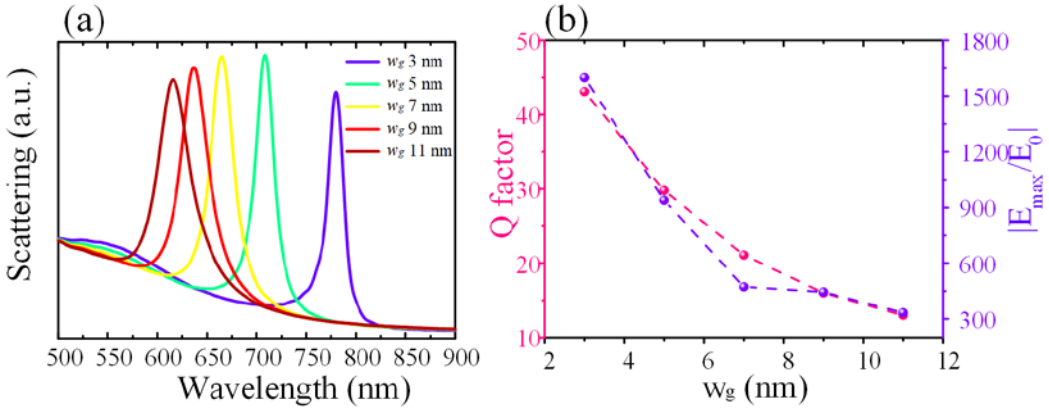

Figure 4. (a) The simulated scattering spectra of the nanoantenna on the silver film with different values of the nanogap. (b) The corresponding Q factor and maximum electric field enhancements of the scattering spectra with different values of the nanogap.

Local electric field enhancement is important to realize strong coupling between light and matter. Then the effects of the size of nanogap on Q factor and local electric field enhancements were numerical studied and the results were shown in Fig. 4. Figure 4(a) is the dependence of the calculated scattering spectra on the excitation wavelength and the nanogap size wg (from 3 nm to 11 nm). When wg increases from 3 nm to 11 nm, one can clearly see that the linewidth of the resonance all increases and that the resonance exhibits a blueshift. This means that the corresponding Q factor decreases with the size of the nanogap wg increases. The obtained Q factors and maximum electric field enhancement ($|E_{max}/E_0|$) for different nanogap size wg are depicted in Fig. 4(b). When w_g is 3 nm, the Q factor of the resonance is 43.1 and the maximum electric field enhancement can be as high as 1599. The Q factor and maximum electric field enhancement then decreases with wg increases. For example, when w_g is 11 nm, the Q factor reaches only 13.9 and maximum electric field enhancement is 334. Therefore, one can vary the size of the nanogap to study the light and matter interactions in the nanogap of the sliver nanoantenna.

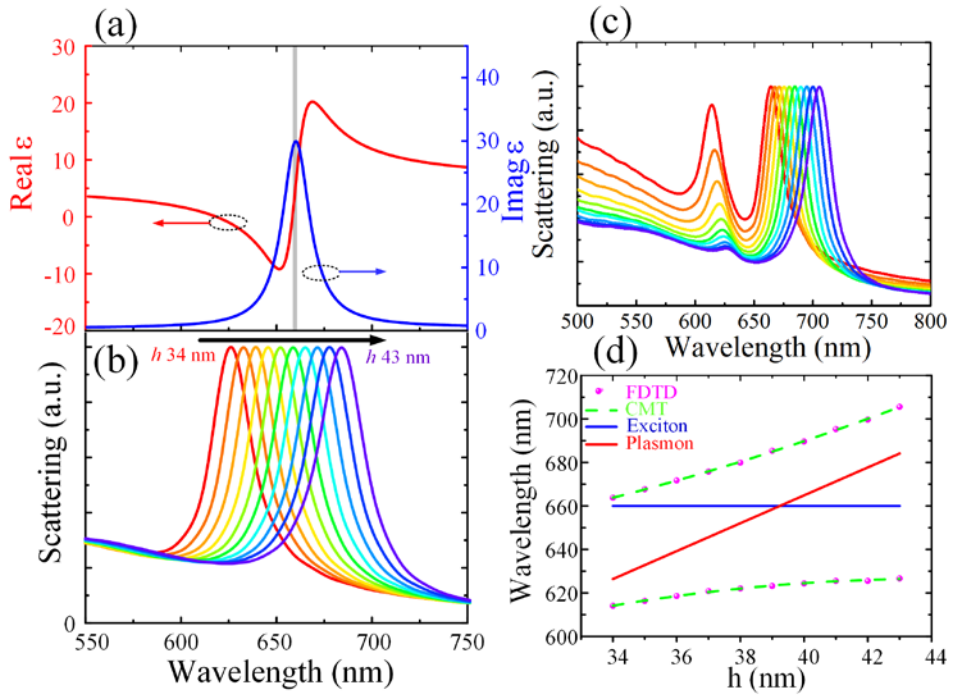

 doi:10.20944/preprints202203.0090.v1

Figure 5. (a) The real (red line) and imaginary (blue line) parts of the relative permittivity of the single QD used in this work. (b) Simulated scattering spectra for different values of thickness h of the silver nanoantenna placed on the silver film. (c) Simulated scattering spectra for different thickness h of the silver nanoantenna coupled with the single QD in the nanogap. (d) The wavelengths of the two new coupling states as the silver nanoantenna thickness h varies. The purple dots and green dashed curve correspond to the FDTD simulation and CMT results, respectively. The blue and red curves represent the individual resonances of the exciton and plasmon modes, respectively.

3.2. Strong coupling between the antenna and single QD.

In this work, the QD with exciton transition at 660 nm was modeled by a Lorentz oscillator model, which was described detailed in the Materials and Methods. Then calculated permittivity of the QD is shown in Fig. 5(a) where a sharp increase in the imaginary part (blue line) can be seen around the exciton resonance at 660 nm (1.879 eV). A series of silver nanoantennas were designed with thickness h ranging from 34 nm to 43 nm in 1 nm steps, in order to tune the bare plasmon resonance from approximately 627 nm to 684 nm, covering the exciton resonance of QD. Figure 5(b) shows the scattering spectra of the silver nanoantenna with different thickness. It can be found that the scattering spectra shows a redshift while the Q factor remains unchanged when the thickness increases from 34 nm to 43 nm.

When the resonance of the plasmon mode is tuned to approach the exciton (660 nm) of the QD, it is possible to achieve strong coupling between the plasmon mode in the silver nanoantenna placed on silver film and excitons in the QD. As shown in Fig. 1, then a single QD with diameter of 6 nm was inset into top center of the nanogap, which has great electric field enhancements. Two methods can be utilized to inset single QD into the nanocavity. One is using interfacial capillary forces to drive the QDs even to single limit into the nanogaps by Santhosh *et al*[26]. The other is taking advantage of atomic force microscopy (AFM) to manipulate single QD into the nanocavity[29, 30]. Figure 5(c) shows scattering spectra of the hybrid structure with different silver nanoantenna thickness h. As the curves in Fig. 5(b) show, the resonant wavelength of the plasmon mode increases with increasing thickness *h*. However, the exciton resonance of the QD remains unchanged. As the thickness *h* increases, the resonant wavelength of the plasmon mode will shift across the exciton resonant wavelength. As can be seen in Fig. 5(c), all scattering spectra show a clear mode splitting with two new peaks and one dip, which are different from the individual plasmon and exciton resonances. The scattering peaks are the result of the strong light and matter interactions between the plasmon and exciton resonances.

The wavelengths of two new coupling states as a function of silver nanoantenna thickness h. The purple dots and green dashed curve correspond to FDTD simulation and CMT results, respectively. The blue and red curves represent the individual resonances of the exciton and plasmon modes, respectively. As can be clearly seen in the scattering spectra in Fig. 5(d), unique anticrossing upper (UB) and lower (LB) bands are obtained. Such anticrossing trend proves the robust nanogap-exciton coupling in the hybrid structure. Coupled mode theory (CMT) was used to describe the two new hybrid states and fitted the exciton-plasmon coupling dispersion. The eigen-energies of the coupling modes ELB,UB are given by[31]:

$$\begin{bmatrix} E_p + i\hbar\gamma_p & g \\ g & E_e + i\hbar\gamma_e \end{bmatrix} \begin{bmatrix} \alpha \\ \beta \end{bmatrix} = E_{LB,UB} \begin{bmatrix} \alpha \\ \beta \end{bmatrix} \quad (2)$$

Here, E_p and E_e are the energies for the uncoupled plasmon mode and the exciton resonance, respectively. γ_p and γ_e are the half-bandwidths of the uncoupled plasmon and exciton resonances, respectively. g is the coupling rate characterizing the interaction between the plasmon mode and exciton resonance. α and β are the Hopfield coefficients that meets $|\alpha|^2+|\beta|^2=1$, respectively. Also $|\alpha|^2$ and $|\beta|^2$ represent the fractions of the plasmon mode and excitons in the new hybrid states. The eigenvalues are obtained as:

$$E_{LB,UB} = \frac{1}{2}[E_e + E_p + i(\gamma_e + \gamma_p)/2] \pm \sqrt{g^2 + \frac{1}{4}[E_e - E_p + i(\gamma_p - \gamma_e)]^2} \quad (3)$$

Using Eq. 3, with zero detuning for two new hybrid bands, the Rabi splitting energy of

$$\hbar\Omega = 2\sqrt{g^2 - (\gamma_p - \gamma_e)^2/4} \quad (4)$$

can be obtained from FDTD and CMT fitting results in Fig. 5(d). For strong coupling criteria, one of the following conditions should be satisfied:

$$N_1 = \hbar\Omega/(\gamma_p + \gamma_e) > 1 \text{ and } N_2 = g/\sqrt{(\gamma_e^2 + \gamma_p^2)/2} > 1 \quad (5)$$

In this work, γ_e = 40 meV and γ_p = 42.0 meV. The Rabi splitting $\hbar\Omega$ = 188.0 meV at zero detuning is extracted from FDTD calculated results. An exciton-plasmon interaction strength of g = 100.8 meV was then obtained and thus, from FDTD simulation results, we obtain N_1 = 2.29 and N_2 = 2.46, which can satisfy the strong coupling criteria. By treating g as a free fitting parameter, the dispersion of the exciton-polaritons can be fitted by CMT using Eq. 4, the results of which are plotted as the green dashed curve shown in Fig. 5(d). From the CMT fitting curve, g = 99.5 meV and $\hbar\Omega$ = 185.1 meV are obtained. Then the corresponding N_1 = 2.20 and N_2 = 2.43 will also meet the strong coupling criteria. Therefore, both CMT and FDTD results suggest that the criterion for strong coupling is satisfied. Strong coupling between the plasmon mode and excitons is also confirmed. In addition, the Rabi splitting $\hbar\Omega$ can be further increased when the QD is inserted very close to the silver nanoantenna.

4. Conclusions

In summary, a plasmonic nanoantenna placed on a metal film, which has ultra-high electric field enhancement and ultra-small optical volume in the nanogap, was designed. When compared with the nanoantenna directly placed on the substrate, the metal film contributes to further increase the local field enhancement. Then strong coupling between the plasmon mode of silver nanoantenna placed on a metal film and excitons in a QD has been investigated both theoretically and numerically, and the FDTD results coincide well with CMT calculations. The simulation results show that strong coupling between the plasmon mode and excitons leads to distinct scattering spectral splitting. Furthermore, anticrossing behavior featured with two new hybrid states can be achieved by varying the thickness of the silver nanoantenna, respectively. The unique optical coupling between the exciton and the plasmon modes can be used to realize strong light–matter interactions in a single quantum emitter, and the hybrid structure designed here will be beneficial to future studies of quantum information operations and other nanophotonics applications.

Author Contributions: Conceptualization, S.C. and S.H.; methodology, S.C.; software, S.C.; validation, Y.S. and Z.L.; writing—original draft preparation, S.C.; writing—review and editing, S.C., Y.S, Z.L. and S.H.; supervision, S.H.; funding acquisition, S.C and S.H. All authors have read and agreed to the published version of the manuscript.

Funding: This work was partially supported by the National Natural Science Foundation of China (No. 62105282, 91833303, 11621101, 61550110246), the National Key Research and Development Program of China (No. 2017YFA0205700, 2018YFC1407503), Ningbo Science and Technology Project (2020Z077, 2018B10093), Key Research and Development Program of Zhejiang Province (2021C03178) and Guangdong Innovative Research Team Program (No. 201001D0104799318).

Data Availability Statement: Not applicable.

Conflicts of Interest: The authors declare no conflict of interest.

References

1. H. Mabuchi, A. Doherty, "Cavity quantum electrodynamics: coherence in context," Science 298, 1372-1377. (2002).
2. J. Kasprzak, M. Richard, S. Kundermann, A. Baas, P. Jeambrun, J.M.J. Keeling, F. Marchetti, M. Szymańska, R. André, J. Staehli, "Bose–Einstein condensation of exciton polaritons," Nature 443, 409-414 (2006).
3. P. Törmä, W.L. Barnes, "Strong coupling between surface plasmon polaritons and emitters: a review," Rep Prog Phys 78, 013901 (2014).
4. H. Shan, Y. Yu, X. Wang, Y. Luo, S. Zu, B. Du, T. Han, B. Li, Y. Li, J. Wu, " Observation of ultrafast plasmonic hot electron transfer in the strong coupling regime," Light: Sci. Appl. 8, 1-9 (2019).
5. K. Hennessy, A. Badolato, M. Winger, D. Gerace, M. Atatüre, S. Gulde, S. Fält, E.L. Hu, A. Imamoğlu, "Quantum nature of a strongly coupled single quantum dot–cavity system," Nature 445, 896-899 (2007).
6. C. Monroe, "Quantum information processing with atoms and photons," Nature 416, 238-246 (2002).
7. H.-K. Lo, H.F. Chau, "Unconditional security of quantum key distribution over arbitrarily long distances," Science 283, 2050-2056 (1999).
8. H.J. Kimble, "The quantum internet," Nature 453, 1023-1030 (2008).
9. S. Kéna-Cohen, S. Forrest, "Room-temperature polariton lasing in an organic single-crystal microcavity," Nat. Photonics 4, 371-375 (2010).
10. W. Chen, K.M. Beck, R. Bücker, M. Gullans, M.D. Lukin, H. Tanji-Suzuki, V. Vuletić, "All-optical switch and transistor gated by one stored photon," Science 341, 768-770 (2013).
11. J.P. Reithmaier, G. Sęk, A. Löffler, C. Hofmann, S. Kuhn, S. Reitzenstein, L. Keldysh, V. Kulakovskii, T. Reinecke, A. Forchel, "Strong coupling in a single quantum dot–semiconductor microcavity system," Nature 432, 197-200 (2004).
12. T. Yoshie, A. Scherer, J. Hendrickson, G. Khitrova, H. Gibbs, G. Rupper, C. Ell, O. Shchekin, D. Deppe, "Vacuum Rabi splitting with a single quantum dot in a photonic crystal nanocavity," Nature 432, 200-203 (2004).
13. L. Zhang, R. Gogna, W. Burg, E. Tutuc, H. Deng, "Photonic-crystal exciton-polaritons in monolayer semiconductors," Nat. Commun. 9, 1-8 (2018).
14. S. Cao, H. Dong, J. He, E. Forsberg, Y. Jin, S. He, "Normal-incidence-excited strong coupling between excitons and symmetry-protected quasi-bound states in the continuum in silicon nitride–WS2 heterostructures at room temperature," J. Phys. Chem. Lett. 11, 4631-4638 (2020).
15. V. Kravtsov, E. Khestanova, F.A. Benimetskiy, T. Ivanova, A.K. Samusev, I.S. Sinev, D. Pidgayko, A.M. Mozharov, I.S. Mukhin, M.S. Lozhkin, "Nonlinear polaritons in a monolayer semiconductor coupled to optical bound states in the continuum," Light: Sci. Appl. 9, 1-8 (2020).
16. S. Cao, Y. Jin, H. Dong, T. Guo, J. He, S. He, "Enhancing single photon emission through quasi-bound states in the continuum of monolithic hexagonal boron nitride metasurface," J. Phys.: Mater. 4, 035001 (2021).
17. S. Wang, S. Li, T. Chervy, A. Shalabney, S. Azzini, E. Orgiu, J.A. Hutchison, C. Genet, P. Samorì, T.W. Ebbesen, "Coherent coupling of WS2 monolayers with metallic photonic nanostructures at room temperature," Nano Lett. 16, 4368-4374 (2016).
18. M.L. Brongersma, V.M. Shalaev, "The case for plasmonics," Science 328, 440-441 (2010).
19. M.H. Griep, N.M. Bedford, "Amino-acid conjugated protein–Au nanoclusters with tuneable fluorescence properties," J. Phys.: Mater. 3, 045002 (2020).
20. Y.-D. Wu, "High efficiency multi-functional all-optical logic gates based on MIM plasmonic waveguide structure with the Kerr-type nonlinear nano-ring resonators," Prog. Electromagn. Res. 170, 79-95 (2021).
21. H. Zhang, J. Sun, J. Yang, I. De Leon, R.P. Zaccaria, H. Qian, H. Chen, G. Wang, T. Wang, "Biosensing performance of a plasmonic-grating-based nanolaser," Prog. Electromagn. Res. 171, 159-169 (2021).
22. A.E. Schlather, N. Large, A.S. Urban, P. Nordlander, N.J. Halas, "Near-field mediated plexcitonic coupling and giant Rabi splitting in individual metallic dimers," Nano Lett. 13, 3281-3286 (2013).
23. G. Zengin, G. Johansson, P. Johansson, T.J. Antosiewicz, M. Käll, T. Shegai, "Approaching the strong coupling limit in single plasmonic nanorods interacting with J-aggregates," Sci. Rep. 3, 1-8 (2013).
24. G. Zengin, M. Wersäll, S. Nilsson, T.J. Antosiewicz, M. Käll, T. Shegai, "Realizing strong light-matter interactions between single-nanoparticle plasmons and molecular excitons at ambient conditions," Phys. Rev. Lett. 114, 157401 (2015).
25. H. Groß, J.M. Hamm, T. Tufarelli, O. Hess, B. Hecht, "Near-field strong coupling of single quantum dots," Science Adv. 4, eaar4906 (2018).

 doi:10.20944/preprints202203.0090.v1

26. K. Santhosh, O. Bitton, L. Chuntonov, G. Haran, "Vacuum Rabi splitting in a plasmonic cavity at the single quantum emitter limit," Nat. Commun. 7, 1-5 (2016).
27. P.B. Johnson, R.-W. Christy, "Optical constants of the noble metals," Phys. Rev. B 6, 4370 (1972).H. Mabuchi, A. Doherty, Cavity quantum electrodynamics: coherence in context, Science, 298 (2002) 1372-1377.
28. G. Zhang, S. Jia, Y. Gu, J. Chen, "Brightening and guiding single-photon emission by plasmonic waveguide–slit structures on a metallic substrate," Laser Photonics Rev. 13, 1900025 (2019).
29. J. Tang, J. Xia, M. Fang, F. Bao, G. Cao, J. Shen, J. Evans, S. He, "Selective far-field addressing of coupled quantum dots in a plasmonic nanocavity," Nat. Commun. 9, 1705 (2018).
30. J. Xia, J. Tang, F. Bao, Y. Sun, M. Fang, G. Cao, J. Evans, S. He, "Turning a hot spot into a cold spot: polarization-controlled Fano-shaped local-field responses probed by a quantum dot," Light: Sci. Appl. 9, 166 (2020).
31. X. Liu, T. Galfsky, Z. Sun, F. Xia, E.-c. Lin, Y.-H. Lee, S. Kéna-Cohen, V.M. Menon, "Strong light–matter coupling in two-dimensional atomic crystals," Nat. Photonics 9, 30-34 (2015).